J Mater Sci (2008) 43:3130–3134
DOI 10.1007/s10853-008-2509-1

Proton conductivity of biopolymer–platinum nanoparticle composite under high humidity

Musashi Fujishima · Hiroaki Takatori · Kasumi Yamai · Yuki Nagao · Hiroshi Kitagawa · Kumao Uchida

Received: 26 October 2007 / Accepted: 29 January 2008 / Published online: 28 February 2008

Abstract A κ-carrageenan–Pt nanoparticle composite (Cg–Pt) was synthesized and its proton conductivity was examined by a complex-plane impedance method. The synthesized Cg–Pt was characterized by transmission electron microscope (TEM) observation, powder X-ray diffraction (XRD), Fourier transformed infrared (FT-IR) absorption measurements, and thermogravimetry/mass spectrometry (TG/MS) analysis. It was revealed that the a.c. electrical conductivity of Cg–Pt strongly depends on relative humidity (RH) and exceeds the conductivity of Cg under conditions of high humidity. From the temperature dependence of the a.c. conductivity, activation energies for protonic conduction were estimated to be 0.47 and 0.34 eV for Cg–Pt and Cg, respectively. The origin of the differences in the conductivities and activation energies are discussed.

Introduction

Polymer-metal nanoparticle composites have attracted much attention of material scientists in hydrogen technology because of their potential applications for hydrogen storage [1–3], hydrogenation of organic substances [4, 5], and photo-catalytic hydrogen production from water [6, 7]. The advantage of composites is that they can be fabricated from a wide variety of metal nanoparticles and polymers by facile synthetic methods, and that their physical properties including electronic and ionic conduction can be controlled by selection of the constituents.

Protonic conduction of the composites is worthy of research in the field of electrolytes and membrane-electrode assemblies (MEA) for polymer electrolyte fuel cells (PEFC) [8]. However, reports on protonic conduction are few in number although electronic conduction of the composites has been studied intensively [9]. The simple method for fabricating proton-conductive composites is the use of polymeric proton conductors as constituents.

Among many kinds of polymeric conductors, we have focused on κ-carrageenan (Cg, Fig. 1), which is an acidic polysaccharide extracted from red seaweed [10]. Cg is composed of alternately repeating units of 4-linked 3,6-anhydro-α-D-galactose and 3-linked β-D-galactose with one sulfate group per disaccharide unit. Cg shows sol–gel transition and forms aggregates of helical structures at room temperature. Cg is a highly proton-conductive material because it possesses the capability of water absorption, which induces dissociation of protons from the acidic groups. Dissociated protons migrate through hydrogen-bonded networks formed with the absorbed water molecules.

In addition, Cg is an environment-friendly, reproducible biopolymer because it is a product of a biological photosynthetic process. Therefore, Cg has industrial advantages such as abundant resources, low energy consumption, low-cost synthesis, carbon neutrality, and harmless disposal. Since these features cannot be realized with conventional perfluoroalkyl sulfonate electrolytes such as a Nafion® membrane, Cg is expected to be an essential constituent of environment-friendly electrolytes and MEA. In this study, we report the preparation of a Cg-platinum nanoparticle composite (Cg–Pt) and its proton conductivity is measured by a complex-plane impedance method.

M. Fujishima (✉) · H. Takatori · K. Yamai · Y. Nagao · H. Kitagawa · K. Uchida
School of Science and Engineering, Kinki University,
3-4-1 Kowakae, Higashi-Osaka, Osaka 577-8502,
Japan
e-mail: mfujishima@apch.kindai.ac.jp

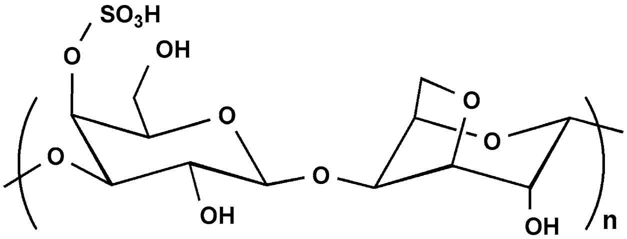

Fig. 1 Molecular structure of κ-carrageenan (Cg)

Experimental

Sample preparation

All chemical reagents were purchased from Wako Pure Chemical Industries Ltd. and used without further purification. At first, Pt nanoparticles were synthesized by reflux of mixed aqueous solution of $H_2PtCl_6 \cdot 6H_2O$ (0.1 mM) and an excess amount of ethanol. A change in the solution color from pale yellow to black was observed in several tens of minutes. The black colloidal dispersion of Pt nanoparticles was then cooled to room temperature, into which an aqueous solution of Cg (1.2 mM) was subsequently added. The mixed dispersion was condensed with a rotary evaporator and dried in vacuo at room temperature. Film samples obtained by this procedure were washed with diethyl ether several times and dried again. The weight fraction of Pt nanoparticles in Cg–Pt is 1.8 wt.%.

Measurements

The synthesized Cg–Pt was observed with a Jeol-3010 TEM in bright-field diffraction contrast mode at an acceleration voltage of 300 kV. The observations were performed using copper grids on which several drops of aqueous dispersions of Cg–Pt were dropped and dried in vacuo. The Pt nanoparticles were characterized by powder X-ray diffraction (XRD) measurements with a Philips X'Pert-MPD diffractometer with Cu Kα radiation and Fourier transformed infrared (FT-IR) absorption measurements with a JASCO FT/IR-470 spectrometer. The thermal stabilities of Cg–Pt and Cg were examined by thermogravimetry/mass spectrometry (TG/MS) analyses with a Bruker TG-DTA/M59610 in the temperature range of 30–290 °C. In the experiments, temperature dependence of the ionic currents from the decomposition products (C, CO_2, and SO_2) was monitored during heating.

The a.c. electrical conductivities of Cg–Pt and Cg were measured with a Hioki 3532-50 LCR HiTester by a conventional quasi-four-probe method using pressed pellets of powdered samples. Complex-plane impedance plots were obtained in the frequency range of 4–5 MHz at 0.1 V. The relative humidity (RH) dependence at 20 °C and temperature dependence at 80% RH of the a.c. conductivities were recorded with a personal computer connected to the HiTester. To determine the conduction carriers, the isotope effect on the a.c. electrical conductivity was investigated. In the experiment, H_2O and D_2O vapors were alternately introduced into the sample container.

Results and discussion

Figure 2 shows a powder XRD pattern of the synthesized Cg–Pt with a pattern of Pt black for comparison. It is obvious that the diffraction pattern of Cg–Pt corresponds well with the pattern of Pt black with respect to their peak positions. In addition, the diffraction peaks of Cg–Pt are much broader than are those of Pt black. These observations mean that Cg–Pt contains fine Pt particles with a face-centered cubic lattice structure. By the Scherrer equation [11], the crystalline size of the particle was estimated to be 4.1 nm.

Figure 3 is a TEM image of Cg–Pt. Although the mean diameter of the Pt nanoparticles could not be estimated because of their aggregation, the diameter of the particles appears to be *ca.* 4 nm. This value is in reasonable agreement with the estimated crystalline size. The aggregation should be caused by the drying treatment of the aqueous dispersion of Cg–Pt in the preparation of the TEM samples.

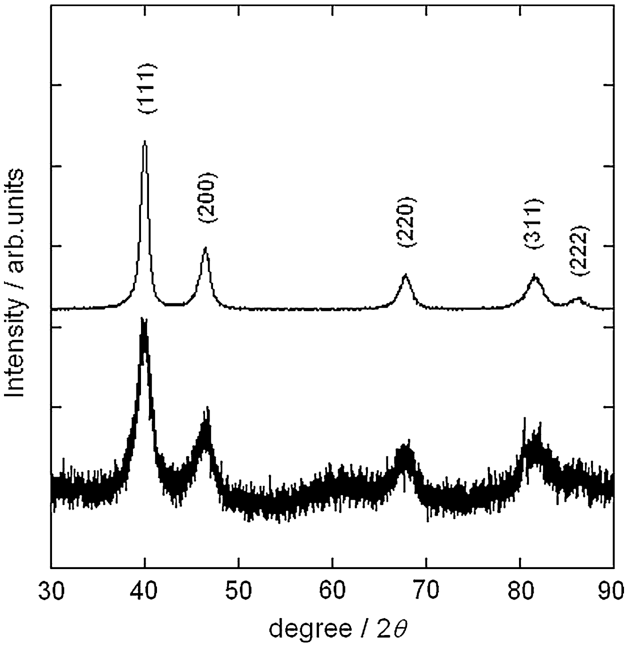

Fig. 2 Powder-XRD patterns of Cg–Pt (bold line) and Pt black (fine line)

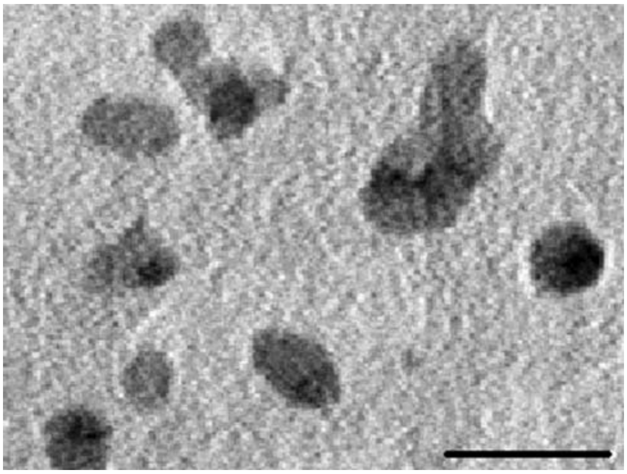

Fig. 3 TEM image of Cg–Pt (scale bar: 10 nm). The sample was observed in bright-field diffraction contrast mode

FT-IR absorption spectra of Cg–Pt and Cg did not show any distinguishable difference in the wavelength region of 400 to 4,000 cm^{-1}. This indicates that Cg is not degraded in the present synthetic procedure. From TG/MS analyses, the increase of the ionic currents of CO_2 was observed at *ca.* 140 and 180°C for Cg–Pt and Cg, respectively. The starting temperature of the increase corresponds to the decomposition temperature of the samples. The lower decomposition temperature for Cg–Pt seems to be caused by the catalytic effect of the Pt nanoparticles.

Figure 4 shows the RH dependences of a.c. electrical conductivities at 20 °C. The a.c. conductivity for Cg–Pt was increased by about five orders of magnitude from 1.59×10^{-8} to 8.19×10^{-4} Scm^{-1} with an increase of RH from 40 to 90% RH. The a.c. conductivity for Cg was also increased in the same RH region. Such strong RH dependence shows similar behavior to the a.c. conductivities of highly proton-conductive polymers such as a humidified Nafion® membrane. It is noteworthy that the a.c. conductivity of Cg–Pt is higher than the conductivity of Cg under high humidity conditions (>50% RH).

To determine conduction carriers, the isotope effect on a.c. conductivity was investigated. Figure 5 shows transients of a.c. electrical conductivity of Cg–Pt under H_2O and D_2O vapor condition. The a.c. conductivity was observed to be increased by the introduction of H_2O vapor but decreased by the introduction of D_2O vapor. This phenomenon comes from the difference in ionic mobility between proton and deuteron. This observation clearly suggests that conduction carriers in Cg–Pt are protons, which should migrate through hydrogen-bonded networks formed by absorbed water molecules.

Figure 6 shows Arrhenius plots of a.c. electrical conductivities at 80% RH between 10 and 50 °C. It can be seen that the conductivity of Cg–Pt is higher than that of Cg in this temperature range. In addition, the increasing rate of the former with an increase of temperature appears to be slightly larger than the rate of the latter. The linearly increasing a.c. conductivities indicate that the proton migration is of the thermal activation type. In general, proton migration of this type obeys Nernst–Einstein law as the following form [12]:

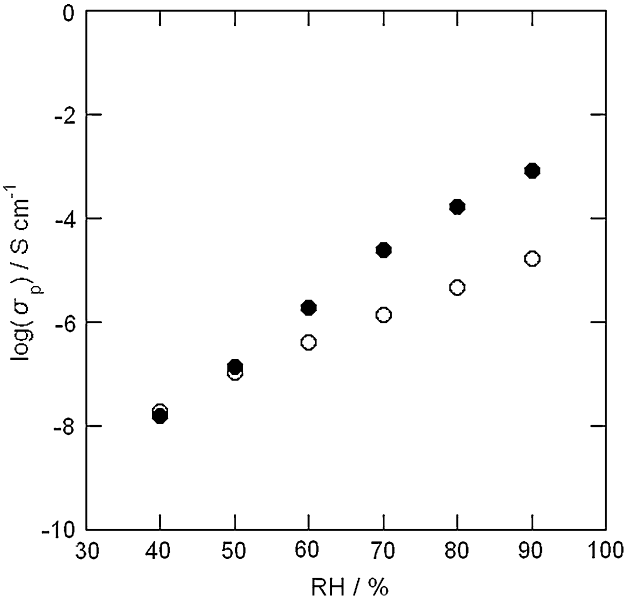

Fig. 4 RH dependence of a.c. electrical conductivities of Cg–Pt (solid circle) and Cg (open circle)

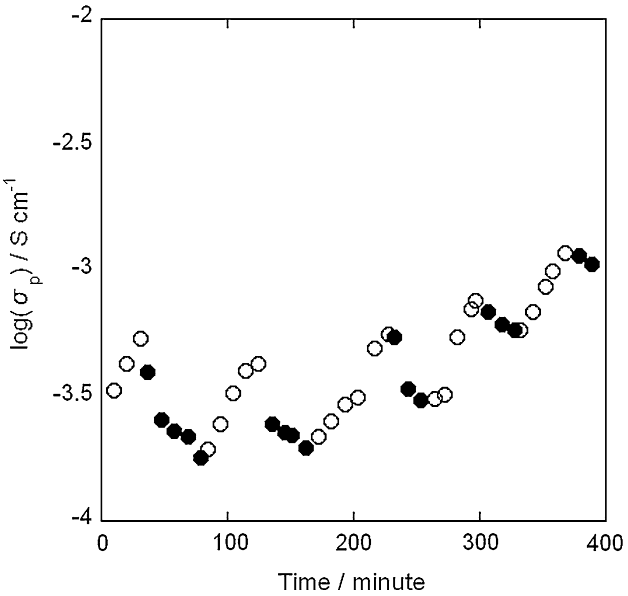

Fig. 5 The a.c. electrical conductivity under D_2O (solid circle) and H_2O (open circle) vapor conditions

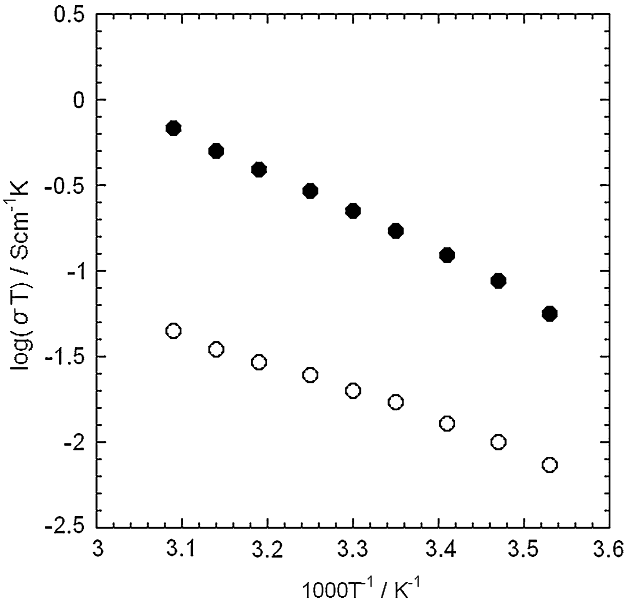

Fig. 6 Temperature dependence of a.c. electrical conductivities of Cg–Pt (solid circle) and Cg (open circle)

$$\sigma = (DCe^2)/kT \tag{1}$$

$$D = D_0 \exp(-E_a/kT) \tag{2}$$

where D is the diffusion coefficient, C is the concentration of mobile ions, e is the charge of mobile ions, k is the Boltzmann constant, T is the temperature, and E_a is the activation energy. From these equations, E_a for Cg–Pt and Cg were estimated to be 0.47 and 0.34 eV, respectively. These values represent the difference in the increasing rate of the conductivity between Cg–Pt and Cg.

The difference in the proton conductivities and activation energies is considered to result from the incorporation of Pt nanoparticles with Cg. It is well known that incorporation of inorganic particles into ion-conductive matrixes enhances ionic conductivity [13]. In the literature, this phenomenon was explained by an accumulation of ionic species in the space-charge layer formed at the particle-matrix interface. In this mechanism, the enhancement of ionic conduction occurs depending on particle fractions in the matrix. In a certain fraction, an ion-conductive pathway is constructed by the overlapping of the space-charge layers.

This mechanism is applicable to the enhanced proton conductivity for Cg–Pt because Pt nanoparticles tend to have a negative charge under hydrous conditions and attract positively charged ions [14]. That is, the space-charge layer at the Pt nanoparticle–Cg interface should be formed with protons dissociated from sulfate groups under high humidity conditions. As such, the space-charge layers may overlap and, as a result, a proton-conductive pathway with fast proton migration should be formed. The extent of the overlapping should depend on temperature and become larger with an increase of temperature because of the increased thermal diffusivity of protons. Such growth behavior of the proton-conductive pathway may be responsible for the larger increasing rate of the conductivity, i.e., larger activation energy, for Cg–Pt.

In addition to the effect of the space-charge layer, it is known that an increase in the mobility of polymer chains also enhances the migration of ions [15]. This mechanism also seems to be true for the enhanced proton conductivity of Cg–Pt. The reason is that the incorporation of Pt nanoparticles with Cg and the humidification influence the formation of the superstructure of Cg through an inhibition in the reorganization of the polymer chains and an increase in their segmental motions. In practice, the enhanced proton conductivity in this study should be the result of the combined effect of the former and latter mechanisms.

Conclusion

We synthesized a κ-carrageenan–Pt nanoparticle composite and revealed the proton conductivity by their RH and temperature dependences and the isotope effect. Cg–Pt showed higher proton conductivity and larger activation energy than did corresponding values for Cg. The observed enhanced protonic conduction is, to our knowledge, the first observation of this phenomenon in polymer-metal nanoparticle composites. The composites in this study will become highly proton conductive, environment-friendly electrolytes and MEA for PEFC. Detailed investigations of the enhancement effect are now in progress.

Acknowledgements This work was partly supported by a Grant-in-Aid for Scientific Research (No. 17750060) and Nanotechnology Network Project (Kyushu-area Nanotechnology Network) from the Ministry of Education, Culture, Sports, Science and Technology (MEXT), and by the Japan Securities Scholarship Foundation, CASIO Science Promotion Foundation, Kansai Research Foundation for technology promotion, and Nippon Sheet Glass Foundation for Materials Science and Engineering.

References

1. Akiba E (2005) Advanced technologies and materials for hydrogen energy. CMC Publishing, Tokyo
2. Yamauchi M, Kitagawa H (2005) Synth Met 153:353
3. Yamauchi M, Kitagawa H (2005) Chem Eng Trans 8:159
4. Lu P, Teranishi T, Asakura K, Miyake M, Toshima N (1999) J Phys Chem B 103:9673
5. Ohtaki M, Toshima N, Komiyama M, Hirai H (1990) Bull Chem Soc Jpn 63:1433

6. Brugger P-A, Cuendet P, Grätzel M (1981) J Am Chem Soc 103:2923
7. Toshima N, Nakata K, Kitoh H (1997) Inorg Chim Acta 265:149
8. Roeder J, Silva H, Nunes SP, Pires ATN (2005) Solid State Ionics 176:1411
9. Mikrajuddin FG, Shi K, Okuyama J (2000) Electrochem Soc 147:3157
10. Steinbüchel A, Marchessault RH (2005) Biopolymers for medical and pharmaceutical applications. Wiley-VCH, Weinheim
11. Scherrer P (1918) Nachr Gött 2:98
12. Colomban P (1992) Proton conductors solids, membranes and gels—materials and devices. Cambridge University Press, New York
13. Maier J (1995) Prog Solid State Chem 23:171
14. Teranishi T, Hosoe M, Tanaka T, Miyake M (1999) J Phys Chem B 103:3818
15. Croce F, Appetecchi GB, Persi L, Scrosati B (1998) Nature 394:456